Письма в ЭЧАЯ. 2013. Т. 10, № 7(184). С. 1024–1039

ФИЗИКА ЭЛЕМЕНТАРНЫХ ЧАСТИЦ И АТОМНОГО ЯДРА. ТЕОРИЯ

THEORY OF NEUTRINOLESS DOUBLE-BETA DECAY — A BRIEF REVIEW

F. Šimkovic[1]

Joint Institute for Nuclear Research, Dubna

Department of Nuclear Physics and Biophysics, Comenius University, Bratislava

Institute of Experimental and Applied Physics, Czech Technical University, Praha

Neutrinoless double-beta decay ($0\nu\beta\beta$-decay) is a unique probe for lepton number conservation and neutrino properties. This is a process with long and interesting history with important implications for particle physics and cosmology, but its observation is still elusive. The search for the $0\nu\beta\beta$-decay represents the new frontiers of neutrino physics, allowing one to determine the Majorana nature of neutrinos and to fix the neutrino mass scale and possible CP-violation effects, which could explain the matter–antimatter asymmetry in the Universe. At present, a complete theory is missing and, thus, to motivate and guide the experiments, the mechanism mediated by light neutrinos is mostly considered. The subject of interest is an effective mass of Majorana neutrinos, which can be deduced from the measured half-life, once this process is definitely observed. The accuracy of the determination of this quantity is mainly determined by our knowledge of the nuclear matrix elements. There is a request to evaluate them with high precision, accuracy and reliability. Recently, there is an increased interest in the resonant neutrinoless double-electron capture, which may also establish the Majorana nature of neutrinos. This possibility is considered as alternative and complementary to searches for the $0\nu\beta\beta$-decay.

Безнейтринный двойной бета-распад ($0\nu\beta\beta$-распад) является уникальным процессом, чувствительным к закону сохранения лептонного числа и свойствам нейтрино. Этот процесс с богатой и интересной историей, имеющий большое значение для физики элементарных частиц и космологии, до сих пор не был обнаружен экспериментально. Поиски $0\nu\beta\beta$-распада представляют новые передовые исследования в области физики нейтрино, позволяющие установить природу майорановского нейтрино, измерить абсолютное значение масс нейтрино, проверить вероятное CP-нарушение в лептонном секторе, которое, в свою очередь, могло бы объяснить асимметрию вещества и антивещества во Вселенной. В настоящее время отсутствует полная теория безнейтринного двойного бета-распада, и для экспериментальной мотивации в основном рассматриваются механизмы с участием легких нейтрино. Предметом изучения являются эффективные массы майорановских нейтрино, которые могут быть извлечены из значения периода полураспада радиоактивных изотопов в случае наблюдения таких реакций. Точность определения этих величин определяется главным образом из наших знаний о матричных элементах этих ядерных процессов. Определяющим фактором является требование расчетов с высокой теоретической точностью. В последнее время наблюдается повышенный интерес к резонансному безнейтринному двойному электронному захвату, который также может установить природу майорановского нейтрино. Эта возможность рассматривается в качестве альтернативной к поискам $0\nu\beta\beta$-распада.

PACS: 23.40.Hc; 21.60.Jz; 14.60.St; 12.60.Jv

[1]E-mail: simkovic@theor.jinr.ru

INTRODUCTION

After about six decades since the discovery of the neutrino, we have started to understand the role of neutrinos in our world. The discoveries of oscillations of atmospheric, solar, accelerator and reactor neutrinos have opened a new excited era in neutrino physics and represents a big step forward in our knowledge of neutrino properties. The observed small neutrino masses have profound implications for our understanding of the Universe and are now a major focus in astro-, particle and nuclear physics and in cosmology. The physics community worldwide is embarking on the challenging problem, finding whether neutrinos are indeed Majorana particles (i.e., identical to its own antiparticle) as many particle models suggest or Dirac particles (i.e., different from its antiparticle).

The best sensitivity on Majorana nature of neutrinos and small neutrino masses can be reached in the investigation of neutrinoless double-beta decay ($0\nu\beta\beta$-decay) [1, 2],

$$(A, Z) \to (A, Z + 2) + e^- + e^- \tag{1}$$

and the resonant neutrinoless double-electron capture (0νECEC) [2, 3],

$$e_b^- + e_b^- + (A, Z) \to (A, Z - 2)^{**}. \tag{2}$$

A double asterisk in Eq. (2) means that, in general, the final atom $(A, Z - 2)$ is excited with respect to both the electron shell, due to formation of two vacancies for the electrons, and the nucleus. Observing the $0\nu\beta\beta$-decay and/or 0νECEC would tell us that the total lepton number is not a conserved quantity and that neutrinos are massive Majorana fermions.

There are other total lepton number violating nuclear processes, which observation might prove the Majorana nature of masssive neutrinos. For a bound muon in an atom the neutrinoless muon to positron conversion [4],

$$\mu_b^- + (A, Z) \to (A, Z - 2) + e^+, \tag{3}$$

is not hindered by energy conservation in any nuclear system. However, the muonic analog of the $0\nu\beta\beta$-decay [5],

$$\mu_b^- + (A, Z) \to (A, Z - 2) + \mu^+, \tag{4}$$

can be studied only for three isobars (^{44}Ti, ^{72}Se and ^{82}Sr). The sensitivity of these processes to a signal of lepton number violation cannot compete with those of the $0\nu\beta\beta$-decay and the 0νECEC. It is because the number of mesoatoms produced with high-intensity muon beams is significantly less when compared with the number of stable isotopes in the $0\nu\beta\beta$-decay or the 0νECEC experiments.

The $0\nu\beta\beta$-decay and the 0νECEC have not yet been found [6]. The strongest limits on the half-life $T_{1/2}^{0\nu}$ of the $0\nu\beta\beta$-decay were set in Heidelberg–Moscow (^{76}Ge, $1.9 \cdot 10^{25}$ y) [7], NEMO3 (^{100}Mo, $1.0 \cdot 10^{24}$ y) [8], CUORICINO (^{130}Te, $3.0 \cdot 10^{24}$ y) [9], KamLAND-Zen (^{136}Xe, $5.7 \cdot 10^{24}$ y) [10] and EXO experiments (^{136}Xe, $1.6 \cdot 10^{25}$ y) [11] experiments. However, there is an unconfirmed, but not refuted, claim of evidence for neutrinoless double decay in ^{76}Ge by some participants of the Heidelberg–Moscow collaboration [12] with half-life $T_{1/2}^{0\nu} = 2.23^{+0.44}_{-0.31} \cdot 10^{25}$ y. Recently, by a detailed statistical analysis favored and disfavored ranges at 90% C.L. for each nucleus and for couples of nuclei were worked out. It was found that in order to close the region currently allowed at 90% C.L. by the ^{76}Ge claim and by the ^{136}Xe limit, one should cover either the range $T^{0\nu}_{1/2}(^{76}\mathrm{Ge}) \simeq (2.0-2.9)\cdot 10^{25}$ y or the range $T^{0\nu}_{1/2}(^{136}\mathrm{Xe}) \simeq (3.4-4.3)\cdot 10^{25}$ y; alternatively, using a third nucleus such as ^{130}Te, one should cover $T^{0\nu}_{1/2}(^{130}\mathrm{Te}) \simeq (0.7-1.1)\cdot 10^{25}$ y [13].

The main aim of experiments on the search for $0\nu\beta\beta$-decay is the measurement of the effective Majorana neutrino mass $m_{\beta\beta}$,

$$m_{\beta\beta} = \sum_j U^2_{ej} m_j, \tag{5}$$

where U_{ej} is the element of Pontecorvo–Maki–Nakagawa–Sakata (PMNS) unitary mixing matrix [14], and m_j is the mass of neutrino.

The effective Majorana neutrino mass can be calculated by using neutrino oscillation parameters: an assumption about the mass of lightest neutrino, by choosing a type of spectrum (normal or inverted) and values of CP-violating phases. In future experiments [1, 2], a sensitivity

$$|m_{\beta\beta}| \simeq \text{a few tens of meV} \tag{6}$$

is planned to be reached. This is the region of the inverted hierarchy of neutrino masses. In the case of the normal mass hierarchy $|m_{\beta\beta}|$ is too small, a few meV, to be probed in the $0\nu\beta\beta$-decay experiments of the next generation.

To interpret the data from the $0\nu\beta\beta$-decay and the 0νECEC (neutrinoless double electron capture) accurately, a better understanding of the nuclear structure effects important for the description of the nuclear matrix elements (NMEs) is needed. In this connection it is crucial to develop and advance theoretical methods capable of evaluating reliably NMEs, and to realistically assess their uncertainties.

1. THE EFFECTIVE MASS OF MAJORANA NEUTRINOS

The discovery of neutrino oscillations in the SuperKamiokande (atmospheric neutrinos) [15], SNO (solar neutrinos) [16], KamLAND (reactor neutrinos) [17], MINOS [18] (accelerator neutrinos), and other neutrino experiments gives us compelling evidence that neutrinos possess small masses and flavor neutrino fields are mixed. All existing neutrino oscillation data (with the exception of the LSND [19], MiniBooNE [20], short baseline reactor [21], and Gallium [22]) anomalies) are perfectly described by the minimal scheme of three-neutrino mixing. Neutrino flavor states $|\nu_\alpha\rangle$ ($\alpha = e,\ \mu,\ \tau$) are connected to the states of neutrinos with masses m_j ($|\nu_j\rangle$) by the following standard mixing relation:

$$|\nu_\alpha\rangle = \sum_{j=1}^{3} U^*_{\alpha j}|\nu_j\rangle \qquad (\alpha = e,\ \mu, \tau). \tag{7}$$

In the case of Dirac neutrinos the unitary 3×3 PMNS neutrino mixing matrix can be parameterized as follows:

$$U = R_{23}\tilde{R}_{13}R_{12}, \tag{8}$$

where the matrices R_{ij} are rotations in ij space, i.e.,

$$R_{23} = \begin{pmatrix} 1 & 0 & 0 \\ 0 & c_{12} & s_{12} \\ 0 & -s_{12} & c_{12} \end{pmatrix}, \quad \tilde{R}_{13} = \begin{pmatrix} c_{13} & 0 & s_{13}\,\mathrm{e}^{-i\delta} \\ 0 & 1 & 0 \\ -s_{13}\,\mathrm{e}^{i\delta} & 0 & c_{13} \end{pmatrix},$$
$$R_{12} = \begin{pmatrix} c_{12} & s_{12} & 0 \\ -s_{12} & c_{12} & 0 \\ 0 & 0 & 1 \end{pmatrix}, \tag{9}$$

where $c_{ij} \equiv \cos\theta_{ij}$, $s_{ij} \equiv \sin\theta_{ij}$. The θ_{12}, θ_{13} and θ_{23} are mixing angles and δ is the CP phase. If neutrinos are Majorana particles, the matrix U in Eq. (8) is multiplied by a diagonal phase matrix $\mathrm{P} = \mathrm{diag}\left(\mathrm{e}^{i\alpha_1}, \mathrm{e}^{i\alpha_2}, \mathrm{e}^{i\delta_{13}}\right)$, which contains two additional CP phases α_1 and α_2.

With the discovery of neutrino oscillations we know:

• The values of the large mixing angles θ_{12} and θ_{23}. The value of the relatively small angle θ_{13} measured recently in the Double Chooz [23], the Daya Bay [24] and RENO [25] reactor neutrino experiments.

• The solar and atmospheric mass-squared differences[1] $\Delta m^2_{\text{SUN}} = \Delta m^2_{12}$ and $\Delta m^2_{\text{ATM}} = \Delta m^2_{23}$ (normal spectrum), $\Delta m^2_{\text{ATM}} = -\Delta m^2_{13}$ (inverted spectrum).

We do not know the value of the lightest neutrino mass, the CP phases and the character of the neutrino mass spectrum (normal or inverted).

From the data of the MINOS experiment [18] it was found that $\Delta m^2_{\text{ATM}} = (2.43 \pm 0.13)\cdot 10^{-3}$ eV^2. From the analysis of the KamLAND and solar data it was obtained that $\tan^2\theta_{12} = 0.452^{+0.035}_{-0.033}$ [17]. From the global fit to all data it was inferred that [26] $\Delta m^2_{\text{SUN}} = (7.65^{+0.13}_{-0.20})\cdot 10^{-5}$ eV^2 and $\sin^2\theta_{23} = 0.50^{+0.07}_{-0.06}$. Finally, from the analysis of the Daya Bay [24] and RENO data [25] one obtains $\sin^2 2\theta_{13} = 0.092 \pm 0.016$ (stat.) ± 0.005 (syst.) and $\sin^2 2\theta_{13} = 0.103 \pm 0.013$ (stat.) ± 0.011 (syst.), respectively.

The effective Majorana mass is given by

$$|m_{\beta\beta}| = |c^2_{12}c^2_{13}\,\mathrm{e}^{i\alpha_1} m_1 + s^2_{12}c^2_{13}\,\mathrm{e}^{i\alpha_2} m_2 + s^2_{13} m_3| \tag{10}$$

or by the full expression

$$\begin{aligned} |m_{\beta\beta}|^2 = {} & c^4_{12}c^4_{13}m^2_1 + s^4_{12}c^4_{13}m^2_2 + s^4_{13}m^2_3 + \\ & + 2c^2_{12}s^2_{12}c^4_{13}m_1 m_2 \cos(\alpha_1 - \alpha_2) + \\ & + 2c^2_{12}c^2_{13}s^2_{13}m_1 m_3 \cos\alpha_1 + 2s^2_{12}c^2_{13}s^2_{13}m_2 m_3 \cos\alpha_2. \end{aligned} \tag{11}$$

From this equation it simply follows that the effective Majorana mass depends on the character of the neutrino mass spectrum and three unknown parameters: the lightest neutrino mass and two CP phases.

In the three-neutrino case, two mass spectra are currently possible:

• Normal Spectrum (NS): $m_1 < m_2 < m_3$: $\quad \Delta m^2_{12} \ll \Delta m^2_{23}$. In this case

$$m_2 = \sqrt{\Delta m^2_{\text{SUN}} + m^2_0}, \quad m_3 = \sqrt{\Delta m^2_{\text{ATM}} + \Delta m^2_{\text{SUN}} + m^2_0}$$

with $m_0 = m_1$.

[1]We use the following definition: $\Delta m^2_{ij} = m^2_j - m^2_i$.

• Inverted Spectrum (IS), $m_3 < m_1 < m_2$: $\Delta m^2_{12} \ll |\Delta m^2_{13}|$. We have

$$m_1 = \sqrt{\Delta m^2_{\rm ATM} + m_0^2}, \quad m_2 = \sqrt{\Delta m^2_{\rm ATM} + \Delta m^2_{\rm SUN} + m_0^2}$$

with $m_0 = m_3$.

Here, $m_0 = m_1(m_3)$ is the lightest neutrino mass.

We will consider the following two neutrino mass hierarchies:

1. Normal Hierarchy (NH): $m_1 \ll m_2 \ll m_3$:
In this case for the neutrino masses we have

$$m_1 \ll \sqrt{\Delta m^2_{\rm SUN}}, \quad m_2 \simeq \sqrt{\Delta m^2_{\rm SUN}}, \quad m_3 \simeq \sqrt{\Delta m^2_{\rm ATM}}.$$

Neglecting the negligibly small contribution of m_1, we find

$$\cos\alpha_2 \simeq \frac{|m_{\beta\beta}|^2 - s^4_{12}c^4_{13}\Delta m^2_{\rm SUN} - s^4_{13}\Delta m^2_{\rm ATM}}{2s^2_{12}c^2_{13}s^2_{13}\sqrt{\Delta m^2_{\rm SUN}\Delta m^2_{\rm ATM}}}. \tag{12}$$

For the effective Majorana mass we then have the following range of values:

$$|s^2_{12}c^2_{13}\sqrt{\Delta m^2_{\rm SUN}} - s^2_{13}\sqrt{\Delta m^2_{\rm ATM}}| \leqslant |m_{\beta\beta}| \leqslant s^2_{12}c^2_{13}\sqrt{\Delta m^2_{\rm SUN}} + s^2_{13}\sqrt{\Delta m^2_{\rm ATM}}. \tag{13}$$

Using the best-fit values of the mass squared differences and the mixing angles, we find

$$1.5 \leqslant |m_{\beta\beta}| \leqslant 3.8 \text{ meV}.$$

2. Inverted Hierarchy (IH): $m_3 \ll m_1 < m_2$:
In the IH scenario $m_3 \ll \sqrt{\Delta m^2_{\rm ATM}}$ and $m_1 \simeq m_2 \simeq \sqrt{\Delta m^2_{\rm ATM}}$. We find

$$\cos\alpha_{12} = \frac{|m_{\beta\beta}|^2 - c^4_{13}(1 - 2s^2_{12}c^2_{12})\Delta m^2_{\rm ATM}}{2c^2_{12}s^2_{12}c^4_{13}\Delta m^2_{\rm ATM}}, \tag{14}$$

where $\alpha_{12} = \alpha_1 - \alpha_2$. For the absolute value of the effective Majorana mass we find the range

$$|\cos 2\theta_{12}|c^2_{13}\sqrt{\Delta m^2_{\rm ATM}} \leqslant |m_{\beta\beta}| \leqslant c^2_{13}\sqrt{\Delta m^2_{\rm ATM}}. \tag{15}$$

Using the best-fit values of the parameters, we find the following range for $|m_{\beta\beta}|$ in the case of the IH:

$$18 \leqslant |m_{\beta\beta}| \leqslant 48 \text{ meV}.$$

The absolute value of the neutrino mass can be determined from the precise measurement of the end-point part of the β-spectrum of the tritium [27] and other β-decay measurements [28]. Cosmological observations allow one to infer the sum of the neutrino masses

$$m_{\rm cosmo} = \sum_k^3 m_k. \tag{16}$$

The current limits on $m_{\rm cosmo}$ depend on the type of observations included in the fit [29]. The CMB primordial gives $\leqslant$1.3 eV, CMB+distance $\leqslant$ 0.58 eV, galaxy distribution and lensing of galaxies $\leqslant$ 0.6 eV. On the other hand, the largest photometric red shift survey yields $\leqslant$0.28 eV [30]. It is expected that future cosmological observables will be sensitive to $m_{\rm cosmo}$ in the range 0.05–0.1 eV (see, e.g., the recent summary [29]). Thus, the inverted neutrino mass hierarchy will be tested by future precision cosmology. In the case of the inverted mass hierarchy, we have for the sum of the neutrino masses

$$m_{\rm cosmo} \simeq 2\sqrt{\Delta m^2_{\rm ATM}} \simeq 100 \text{ meV}. \tag{17}$$

So, there is a chance that future cosmological observation apparently could restrict the value of m_0 below 10 meV.

The explanation of the LSND [19], MiniBooNE [20], short baseline reactor [21], and Gallium [22] anomalies requires presence of sterile neutrinos. The $U(4\times 4)$ neutrino mixing matrix for one sterile neutrino $(3+1)$ takes the form [2]

$$U = R_{34}\tilde{R}_{24}\tilde{R}_{14}R_{23}\tilde{R}_{13}R_{12}P. \tag{18}$$

It depends on 6 mixing angles (θ_{14}, θ_{24}, θ_{34}, θ_{12}, θ_{13}, θ_{23}, 3 Dirac (δ_{24}, δ_{14}, δ_{13}) and 3 Majorana (α_1, α_2, α_3) CP-violating phases entering the diagonal P matrix:

$$\mathrm{P} = \mathrm{diag}\left(\mathrm{e}^{i\alpha_1}, \mathrm{e}^{i\alpha_2}, \mathrm{e}^{i(\alpha_3+\delta_{13})}, \mathrm{e}^{i\delta_{14}}\right). \tag{19}$$

Similarly, one can parametrized the $U(5\times 5)$ mixing matrix for two sterile neutrinos $(3+2)$ as (10 mixing angles and $5+4$ CP-violating phases)

$$U = R_{45}\tilde{R}_{35}R_{34}\tilde{R}_{25}\tilde{R}_{24}R_{23}\tilde{R}_{15}\tilde{R}_{14}\tilde{R}_{13}R_{12}P, \tag{20}$$

where $\mathrm{P} = \mathrm{diag}\left(\mathrm{e}^{i\alpha_1}, \mathrm{e}^{i\alpha_2}, \mathrm{e}^{i(\alpha_3+\delta_{13})}, \mathrm{e}^{i(\alpha_4+\delta_{14})}, \mathrm{e}^{i\delta_{15}}\right)$.

For explanation of the Reactor Antineutrino Anomaly [21], heavier neutrinos in comparison with three light neutrinos have been introduced with mass squared difference and mixing as follows [31]:

$$\begin{aligned} \Delta m^2_{41} &= 1.78 \text{ eV}^2, \quad U_{e4} = 0.151 \quad (3+1),\\ \Delta m^2_{41} &= 0.46 \text{ eV}^2, \quad U_{e4} = 0.108,\\ \Delta m^2_{51} &= 0.89 \text{ eV}^2, \quad U_{e5} = 0.124 \quad (3+2). \end{aligned} \tag{21}$$

In the presence of one sterile neutrino, the effective neutrino mass in the $0\nu\beta\beta$-decay is given by [2]

$$|m^{3+1}_{\beta\beta}| = |c^2_{12}c^2_{13}c^2_{14}\,\mathrm{e}^{2i\alpha_1}m_1 + c^2_{13}c^2_{14}s^2_{12}\,\mathrm{e}^{2i\alpha_2}m_2 + c^2_{14}s^2_{13}\,\mathrm{e}^{2i\alpha_3}m_3 + s^2_{14}m_4|. \tag{22}$$

We note that from three additional angles $|m_{\beta\beta}|$ depends only on one of them, namely θ_{14}. If there are two sterile neutrinos, we end up with

$$\begin{aligned} |m^{3+2}_{\beta\beta}| = |c^2_{12}c^2_{13}c^2_{14}c^2_{15}\,\mathrm{e}^{2i\alpha_1}m_1 + c^2_{13}c^2_{14}c^2_{15}s^2_{12}\,\mathrm{e}^{2i\alpha_2}m_2 +\\ + c^2_{14}c^2_{15}s^2_{13}\,\mathrm{e}^{2i\alpha_3}m_3 + c^2_{15}s^2_{14}\,\mathrm{e}^{2i\alpha_4}m_4 + s^2_{15}m_5|. \end{aligned} \tag{23}$$

Due to the extra terms in Eqs. (22) and (23) and their couplings, depending on the extra Majorana phases, the sterile could dominate, increase or deplete $|m_{\beta\beta}|$ [2].

2. THE NEUTRINOLESS DOUBLE-BETA DECAY NUCLEAR MATRIX ELEMENTS

The inverse value of the $0\nu\beta\beta$-decay half-life for a given isotope (A,Z) can be written as

$$\frac{1}{T^{0\nu}_{1/2}} = \left|\frac{m_{\beta\beta}}{m_e}\right|^2 \, |M'^{0\nu}|^2 \, G^{0\nu}(E_0, Z). \tag{24}$$

Here, $G^{0\nu}(E_0,Z)$ and $M'^{0\nu}$ are, respectively, the known phase-space factor (E_0 is the energy release) and the nuclear matrix element, which depends on the nuclear structure of the particular isotopes (A,Z), $(A,Z+1)$ and $(A,Z+2)$ under study. The phase space factor $G^{0\nu}(E_0,Z)$ includes fourth power of unquenched axial-vector coupling constant g_A and the inverse square of the nuclear radius R^{-2}, compensated by the factor R in $M'^{0\nu}$. The assumed value of the nuclear radius is $R = r_0 A^{1/3}$ with $r_0 = 1.2$ fm.

The nuclear matrix element $M'^{0\nu}$ is defined as

$$M'^{0\nu} = \left(\frac{g_A^{\rm eff}}{g_A}\right)^2 M^{0\nu}. \tag{25}$$

Here, $g_A^{\rm eff}$ is the quenched axial-vector coupling constant. This definition of $M'^{0\nu}$ [32] allows one to display the effects of uncertainties in $g_A^{\rm eff}$ and to use the same phase-space factor $G^{0\nu}(E_0,Z)$ when calculating the $0\nu\beta\beta$-decay rate.

The nuclear matrix element $M^{0\nu}$ consists of the Fermi (F), Gamow–Teller (GT) and tensor (T) parts as

$$\begin{aligned} M^{0\nu} &= -\frac{M_F^{0\nu}}{(g_A^{\rm eff})^2} + M_{\rm GT}^{0\nu} - M_T^{0\nu} = \\ &= \langle 0_i^+| \sum_{kl} \tau_k^+ \tau_l^+ \left[-\frac{H_F(r_{kl})}{(g_A^{\rm eff})^2} + H_{\rm GT}(r_{kl})\sigma_{kl} - H_T(r_{kl}) S_{kl}\right] |0_f^+\rangle. \end{aligned} \tag{26}$$

Here

$$S_{kl} = 3(\boldsymbol{\sigma}_k \cdot \hat{\mathbf{r}}_{kl})(\boldsymbol{\sigma}_l \cdot \hat{\mathbf{r}}_{kl}) - \sigma_{kl}, \quad \sigma_{kl} = \boldsymbol{\sigma}_k \cdot \boldsymbol{\sigma}_l. \tag{27}$$

The radial parts of the exchange potentials are

$$H_{F,{\rm GT},T}(r_{kl}) = \frac{2}{\pi} R \int_0^\infty \frac{j_{0,0,2}(q r_{kl}) h_{F,{\rm GT},T}(q^2) q}{q + \overline{E}}\, dq, \tag{28}$$

where R is the nuclear radius and $\overline{E}$ is the average energy of the virtual intermediate states used in the closure approximation. The closure approximation is adopted in all the calculation of the NMEs relevant for $0\nu\beta\beta$-decay with the exception of the QRPA. The functions $h_{F,{\rm GT},T}(q^2)$ are given by [33]

$$\begin{aligned} h_F(q^2) &= f_V^2(q^2), \\ h_{\rm GT}(q^2) &= \frac{2}{3} f_V^2(q^2) \frac{(\mu_p - \mu_n)^2}{(g_A^{\rm eff})^2} \frac{q^2}{4m_p^2} + f_A^2(q^2)\left(1 - \frac{2}{3}\frac{q^2}{q^2 + m_\pi^2} + \frac{1}{3}\frac{q^4}{(q^2+m_\pi^2)^2}\right), \\ h_T(q^2) &= \frac{1}{3} f_V^2(q^2) \frac{(\mu_p - \mu_n)^2}{(g_A^{\rm eff})^2} \frac{q^2}{4m_p^2} + \frac{1}{3} f_A^2(q^2)\left(2\frac{q^2}{(q^2 + m_\pi^2)} - \frac{q^4}{(q^2+m_\pi^2)^2}\right). \end{aligned} \tag{29}$$

For the vector normalized to unity and axial-vector form factors the usual dipole approximation is adopted: $f_V(q^2) = 1/(1+q^2/M_V^2)^2$, $f_A(q^2) = 1/(1+q^2/M_A^2)^2$. $M_V = 850$ MeV, and $M_A = 1086$ MeV. The difference in magnetic moments of proton and neutron is $(\mu_p - \mu_n) = 4.71$, and $g_A = 1.254$ is assumed.

The above definition of the $M_\nu^{0\nu}$ includes contribution of the higher order terms of the nucleon current, and the Goldberger–Treiman PCAC relation, $g_P(q^2) = 2m_p g_A(q^2)/(q^2 + m_\pi^2)$ was employed for the induced pseudoscalar term.

The nuclear matrix elements $M'^{0\nu}$ for the $0\nu\beta\beta$-decay must be evaluated using tools of nuclear structure theory. Unfortunately, there are no observables that could be simply and directly linked to the magnitude of $0\nu\beta\beta$ nuclear matrix elements and that could be used to determine them in an essentially model independent way.

The calculation of the $0\nu\beta\beta$-decay NMEs is a difficult problem because ground and many excited states (if closure approximation is not adopted) of open-shell nuclei with complicated nuclear structure have to be considered. In the last few years the reliability of the calculations has greatly improved. Five different many-body approximate methods have been applied for the calculation of the $0\nu\beta\beta$-decay NME:

1. The Interacting Shell Model (ISM) [34, 35]. The ISM allows one to consider only a limited number of orbits close to the Fermi level, but all possible correlations within the space are included. Proton–proton, neutron–neutron and proton–neutron (isovector and isoscalar) pairing correlations in the valence space are treated exactly. Proton and neutron numbers are conserved and angular momentum conservation is preserved. Multiple correlations are properly described in the laboratory frame. The effective interactions are constructed starting from monopole corrected G matrices, which are further adjusted to describe sets of experimental energy levels. The Strasbourg–Madrid codes can deal with problems involving basis of 10^{11} Slater determinants, using relatively modest computational resources. A good spectroscopy for parent and daughter nuclei is achieved. Due to the significant progress in shell-model configuration mixing approaches, there are now calculations performed with these methods for several nuclei.

2. Quasiparticle Random Phase Approximation (QRPA) [32, 33, 36, 37]. The QRPA has the advantage of large valence space but is not able to comprise all the possible configurations. Usually, single particle states in the Woods–Saxon potential are considered. One is able to include to each orbit in the QRPA model space also the spin-orbit partner, which guarantees that the Ikeda sum rule is fulfilled. This is crucial to describe correctly the Gamow–Teller strength. The proton–proton and neutron–neutron pairings are considered. They are treated in the BCS approximation. Thus, proton and neutron numbers are not exactly conserved. The many-body correlations are treated at the RPA level within the quasiboson approximation. Two-body G-matrix elements, derived from realistic one-boson exchange potentials within the Brueckner theory, are used for the determination of nuclear wave functions.

3. Interacting Boson Model (IBM) [40]. In the IBM the low-lying states of the nucleus are modeled in terms of bosons. The bosons are in either $L = 0$ (s boson) or $L = 2$ (d boson) states. Thus, one is restricted to 0^+ and 2^+ neutron pairs transferring into two protons. The bosons interact through one- and two-body forces giving rise to bosonic wave functions.

4. The Projected Hartree–Fock–Bogoliubov Method (PHFB) [38]. In the PHFB wave functions of good particle number and angular momentum are obtained by projection on the axially symmetric intrinsic HFB states. In applications to the calculation of the $0\nu\beta\beta$-decay NMEs the nuclear Hamiltonian was restricted only to quadrupole interaction. The PHFB is

restricted in its scope. With a real Bogoliubov transformation without parity mixing one can describe only neutron pairs with even angular momentum and positive parity.

5. The Energy Density Functional Method (EDF) [39]. The EDF is considered to be an improvement with respect to the PHFB. The density functional methods based on the Gogny functional are taken into account. The particle number and angular momentum, projection for mother and daughter nuclei is performed and configuration mixing within the generating coordinate method is included. A large single particle basis (11 major oscillator shells) is considered. Results are obtained for all nuclei of experimental interest.

The differences among the listed methods of NME calculations for the $0\nu\beta\beta$-decay are due to the following reasons:

(i) The mean field is used in different ways. As a result, single particle occupancies of individual orbits of various methods differ significantly from each other [42].

(ii) The residual interactions are of various origin and renormalized in different ways.

(iii) Various sizes of the model space are taken into account.

(iv) Different many-body approximations are used in the diagonalization of the nuclear Hamiltonian.

(v) Different types of short-range correlations are considered [41]. Each of the applied methods has some advantages and drawbacks, whose effect in the values of the NME can be sometimes explored. The advantage of the ISM calculations is their full treatment of the nuclear correlations, which tends to diminish the NMEs. On the contrary, the QRPA, the EDF, and the IBM underestimate the multipole correlations in different ways and tend to overestimate the NMEs. The drawback of the ISM is the limited number of orbits in the valence space and as a consequence the violation of Ikeda sum rule and underestimation of the NMEs.

In Table 1, recent results of the different methods are summarized. The presented numbers have been obtained with the unquenched value of the axial coupling constant ($g_A^{\rm eff} = g_A = 1.25$)[1], Miller–Spencer Jastrow short-range correlations [43] (the EDF values are multiplied by 0.80 in order to account for the difference between the unitary correlation operator method (UCOM) and the Jastrow approach [41]), the same nucleon dipole form factors, higher order corrections to the nucleon current and the nuclear radius $R = r_0 A^{1/3}$, with $r_0 = 1.2$ fm (the QRPA values [32] for $r_0 = 1.1$ fm are rescaled with the factor $1.2/1.1$). Thus, the discrepancies among the results of different approaches are solely related to the approximations on which a given nuclear many-body method is based.

Comparing $0\nu\beta\beta$-decay nuclear matrix elements calculated by different methods gives some insight into the advantages or disadvantages of different candidate nuclei. However, matrix elements are not quite the only relevant quantities. Experimentally, half-lives are measured or constrained, and the effective Majorana neutrino mass $m_{\beta\beta}$ is the ultimate goal. For $|m_{\beta\beta}|$ equal to 50 meV the calculated half-lives for double β-decaying nuclei of interest are presented in figure. We see that the spread of half-lives for given isotope is up to the factor of 4–5.

It is worth noticing that due to the theoretical efforts made over the last years the disagreement among different NMEs is now much less severe than it was about a decade before.

[1]A modern value of the axial-vector coupling constant is $g_A = 1.269$. We note that in the referred calculations of the $0\nu\beta\beta$-decay NMEs the previously accepted value $g_A^{\rm eff} = g_A = 1.25$ was assumed.

Table 1. **The NME of the $0\nu\beta\beta$-decay $M_\nu^{0\nu}$ calculated in the framework of different approaches: interacting shell model (ISM) [34, 35], quasiparticle random phase approximation (QRPA) [32, 33, 36, 37], projected Hartree–Fock–Bogoliubov approach (PHFB, PQQ2 parametrization) [38], energy density functional method (EDF) [39] and interacting boson model (IBM) [40]. QRPA(TBC) and QRPA(J) denote QRPA results of Tuebingen–Bratislava–Caltech (TBC) and Jyvaskyla (J) groups, respectively. The Miller–Spencer Jastrow two-nucleon short-range correlations are taken into account. The EDF results are multiplied by 0.80 in order to account for the difference between UCOM and Jastrow [41]. $g_A^{\rm eff} = g_A = 1.25$ and $R = 1.2$ fm $\cdot$ $A^{1/3}$ are assumed**

Transition	$\vert M_\nu^{0\nu}\vert$					
	ISM [34, 35]	QRPA (TBC) [32, 36]	QRPA (J) [37]	IBM-2 [40]	PHFB [38]	EDF [39]
^{48}Ca → ^{48}Ti	0.61, 0.57					1.91
^{76}Ge → ^{72}Se	2.30	4.92	4.72	5.47		3.70
^{82}Se → ^{82}Kr	2.18	4.39	2.77	4.41		3.39
^{96}Zr → ^{96}Mo		1.22	2.45		2.78	4.54
^{100}Mo → ^{100}Ru		3.64	2.91	3.73	6.55	4.08
^{110}Pd → ^{110}Cd			3.86			
^{116}Cd → ^{116}Sn		2.99	3.17			3.80
^{124}Sn → ^{124}Te	2.10		2.65			3.87
^{128}Te → ^{128}Xe	2.34	3.97	3.56	4.52	3.89	3.30
^{130}Te → ^{130}Xe	2.12	3.56	3.28	4.06	4.36	4.12
^{136}Xe → ^{136}Ba	1.76	2.30	2.54			3.38
^{150}Nd → ^{150}Sm		3.16		2.32	3.16	1.37

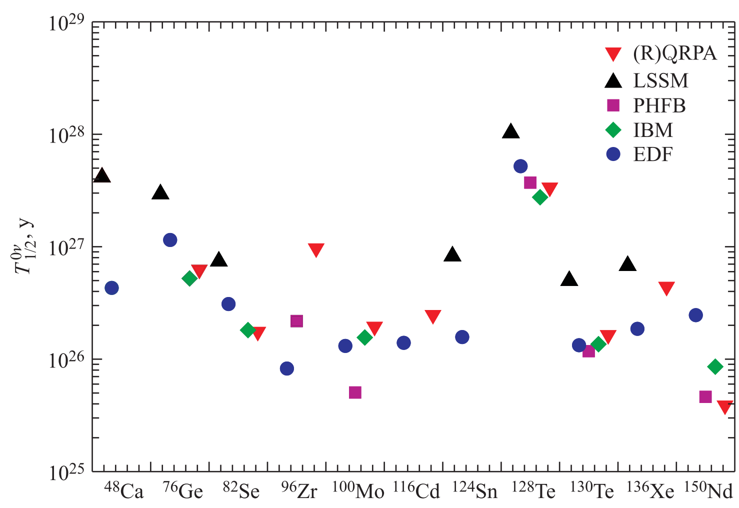

(Color online.) The $0\nu\beta\beta$-decay half-lives of nuclei of experimental interest for $|m_{\beta\beta}| = 50$ meV and NMEs of different approaches. The Miller–Spencer Jastrow two-nucleon short-range correlations are considered. The axial-vector coupling constant g_A is assumed to be 1.25

Nevertheless, the present-day situation with the calculation of $0\nu\beta\beta$-decay NMEs cannot be considered as completely satisfactory. Further progress is required and it is believed that the situation will be improved with time. Accurate determination of the NMEs, and a realistic estimate of their uncertainty, is of great importance. Nuclear matrix elements need to be evaluated with uncertainty of less than 30% to establish the neutrino mass spectrum and CP-violating phases of the neutrino mixing.

3. THE RESONANT NEUTRINOLESS DOUBLE-ELECTRON CAPTURE

The search for the neutrinoless double-electron capture can be a good alternative to the $0\nu\beta\beta$-decay in shedding light on such aspects of neutrino physics as the neutrino type, non-conservation of the total lepton charge and magnitude of the effective Majorana neutrino mass. The probability of neutrinoless double-electron capture can be resonantly enhanced by some orders of magnitude. Although the phenomenon of the resonant enhancement was predicted some decades ago [44–47], the search for resonantly enhanced neutrinoless double-electron-capture transitions was hampered by a lack of precise experimental values of the atomic mass differences of the transition initial and final states. Progress in precision measurement of atomic masses with Penning traps [48] has revived the interest in the old idea on the resonance 0νECEC capture.

Recently, a significant progress has been achieved also in theoretical description of the resonant 0νECEC in [49]. A new theoretical framework for the calculation of resonant 0νECEC transitions, namely, the oscillation of stable and quasi-stationary atoms due to weak interaction with violation of the total lepton number and parity, was proposed in [49]. The 0νECEC-transition rate near the resonance is of Breit–Wigner form,

$$\Gamma^{0\nu\mathrm{ECEC}}_{ab}(J^\pi) = \frac{|V_{ab}(J^\pi)|^2}{\Delta^2 + \frac{1}{4}\Gamma^2_{ab}}\Gamma_{ab}, \tag{30}$$

where J^π denotes angular momentum and parity of final nucleus. The degeneracy parameter can be expressed as $\Delta = Q - B_{ab} - E_\gamma$. Q stands for a difference between the initial and final atomic masses in ground states and E_γ is an excitation energy of the daughter nucleus. $B_{ab} = E_a + E_b + E_C$ is the energy of two electron holes, whose quantum numbers (n, j, l) are denoted by indices a and b and E_C is the interaction energy of the two holes. The width of the excited final atom with the electron holes is given by

$$\Gamma_{ab} = \Gamma_a + \Gamma_b + \Gamma^*. \tag{31}$$

Here, $\Gamma_{a,b}$ is one-hole atomic width and Γ^* is the de-excitation width of daughter nucleus, which can be neglected. Numerical values of Γ_{ab} are about up to few tens of eV.

For light neutrino mass mechanism and favorable cases of a capture of $s_{1/2}$ and $p_{1/2}$ electrons, the explicit form of lepton number violating amplitude associated with nuclear transitions $0^+ \to J^\pi = 0^{\pm 1}, 1^{\pm 1}$ is given in [49]. By factorizing the electron shell structure and nuclear matrix element, one gets

$$V_{ab}(J^\pi) = \frac{1}{4\pi}\; m_{\beta\beta} G^2_\beta \frac{g^2_A}{R} \langle F_{ab}\rangle M^{0\nu\mathrm{ECEC}}(J^\pi). \tag{32}$$

Here, $m_{\beta\beta}$ is the effective mass of Majorana neutrinos, $\langle F_{ab} \rangle$ is a combination of averaged upper and lower bispinor components of the atomic electron wave functions, and $M^{0\nu\mathrm{ECEC}}(J^\pi)$ is the nuclear matrix element (NME). We note that by neglecting the lower bispinor components $M^{0\nu\mathrm{ECEC}}(0^+)$ takes the form of the $0\nu\beta\beta$-decay NME for ground state to ground state transition after replacing isospin operators τ^- by τ^+.

New important theoretical findings with respect of the 0νECEC were achieved in [49]. They are as follows: i) Effects associated with the relativistic structure of the electron shells reduce the 0νECEC half-lives by almost one order of magnitude. ii) The capture of electrons from the $np_{1/2}$ states is only moderately suppressed in comparison with the capture from the $ns_{1/2}$ states unlike in the nonrelativistic theory. iii) For light neutrino mass mechanism selection rules appear to require that nuclear transitions with a change in the nuclear spin $J \geqslant 2$ are strongly suppressed. iv) New transitions due to the violation of parity in the 0νECEC process were proposed. For example, nuclear transitions $0^+ \to 0^\pm, 1^\pm$ are compatible with a mixed capture of s- and p-wave electrons. v) The interaction energy of the two holes E_C has to be taken into account by evaluating a mass degeneracy of initial and final atoms. vi) Based on the most recent atomic and nuclear data and by assuming $M^{0\nu\mathrm{ECEC}}(J^\pi) = 6$, the 0νECEC half-lives were evaluated and the complete list of the most perspective isotopes for further experimental study was provided. Some isotopes such as ^{156}Dy have several closely lying resonance levels. A more accurate measurement of Q-value of ^{156}Dy by Heidelberg group confirmed the existence of multiple-resonance phenomenon for this isotope [50]. vii) In the unitary limit some 0νECEC half-lives were predicted to be significantly below the $0\nu\beta\beta$-decay half-lives for the same value of $|m_{\beta\beta}|$. A probability of finding resonant transition with low 0νECEC half-life was evaluated. viii) The process of the resonant neutrinoless double-electron production (0νEPEP), i.e., neutrinoless double-beta decay to two bound electrons, namely,

$$(A, Z) \to (A, Z + 2)^{**} + e_b^- + e_b^-, \tag{33}$$

was proposed and analyzed. This process was found to be unlikely as it requires that a Q-value is extremely fine tuned to a nuclear excitation. The two electrons must be placed into any of the upper most nonoccupied electron shells of the final atom leaving only restricted possibility to match to a resonance condition.

The probability of the 0νECEC is increased by many orders of magnitude provided the resonance condition is satisfied within a few tens of electron-volts. For a long time there was no way to identify promising isotopes for experimental search of 0νECEC, because of poor experimental accuracy of measurement of Q-values of the order of 1–10 keV for medium heavy nuclei. Progress in precision measurement of atomic masses with Penning traps [50,51] has revived the interest in the old idea on the resonance 0νECEC. The accuracy of Q-values at around 100 eV was achieved. The estimates of the 0νECEC half-lives were recently improved by more accurate measurements of Q-values for ^{74}Se, ^{96}Ru, ^{106}Cd, ^{102}Pd, ^{112}Sn, ^{120}Te, ^{136}Ce, ^{144}Sm, ^{152}Gd, ^{156}Dy, ^{162}Er, ^{164}Er, ^{168}Yb and ^{180}W. It allowed one to exclude some of isotopes from the list of the most promising candidates (e.g., ^{112}Sn, ^{164}Er, ^{180}W) for searching the 0νECEC.

Among the promising isotopes, ^{152}Gd has likely resonance transitions to the 0^+ ground states of the final nucleus as it follows from improved measurement of Q-value for this transition with accuracy of about 100 eV [50]. A detailed calculation of the 0νECEC of $^{152}\mathrm{Gd}$ was performed in [52, 53]. The atomic electron wave functions were treated in the relativistic Dirac–Hartree–Fock approximation. The NME for ground state to ground state transition $^{152}\mathrm{Gd} \to {}^{152}\mathrm{Sm}$ was calculated within the proton–neutron deformed QRPA with a realistic residual interaction [53]. For the favored capture of electrons from K and L shells in the case of ^{152}Gd, the 0νECEC half-life is in the range $4.7 \cdot 10^{28}$–$4.8 \cdot 10^{29}$ y by assuming $|m_{\beta\beta}| = 50$ meV. This transition is still rather far from the resonant level. Currently, the 0νECEC half-life of ^{152}Gd is 2–3 orders of magnitude longer than the half-life of $0\nu\beta\beta$-decay of ^{76}Ge corresponding to the same value of $|m_{\beta\beta}|$ and is the smallest known half-life among known 0νECEC.

Observing the $0\nu\beta\beta$-decay and/or 0νECEC would tell us that the total lepton number is not a conserved quantity and that neutrinos are massive Majorana fermions. There is an increased experimental activity in the field of the resonant 0νECEC [54,55]. The resonant 0νECEC has some important advantages with respect to experimental signatures and background conditions. The de-excitation of the final excited nucleus proceeds in most cases through a cascade of easy to detect rays. A two- or even higher-fold coincidence setup can cut down any background rate right from the beginning, thereby requiring significantly less active or passive shielding. A clear detection of these γ rays would already signal the resonant 0νECEC without any doubt, as there are no background processes feeding those particular nuclear levels. It is worth noting that lepton number conserving ECEC with emission of two neutrinos is strongly suppressed due to almost vanishing phase space [49]. The ground state to ground state resonant 0νECEC transitions can be detected by monitoring the X rays or Auger electrons

Table 2. **A comparison of the neutrinoless double-beta decay and the resonant neutrinoless double-electron capture for light neutrino mass mechanism. The lepton number violating amplitude $V_{ab}(J^\pi)$ is given in Eq. (32)**

	$0\nu\beta\beta$-decay	0νECEC
Definition	$(A,Z) \to (A,Z+2) + e^- + e^-$	$(A,Z) + e_b^- + e_b^- \to (A,Z-2)^{**}$
Formalism	Perturbation field theory	Oscillation of atoms [49]
Half-life	$\frac{1}{T_{1/2}^{0\nu}} = \left\lvert\frac{m_{\beta\beta}}{m_e}\right\rvert^2 G^{0\nu} \lvert M^{0\nu}(J^\pi)\rvert^2$	$\frac{\ln 2}{T_{1/2}^{0\nu\mathrm{ECEC}}} = \frac{\lvert V_{ab}(J^\pi)\rvert^2}{(M_{A,Z} - M^{**}_{A,Z-2})^2 + \frac{1}{4}\Gamma^2_{ab}}\Gamma_{ab}$
Nucl. trans.	$0^+ \to 0^+, 2^+$	$0^+ \to 0^+, 0^-, 1^+, 1^-$
fav. at. syst.	Large Q-value (3–4 MeV) ^{48}Ca, ^{76}Ge, ^{76}Se, ^{100}Mo, ^{116}Cd, ^{130}Te, ^{136}Xe, ^{150}Nd	Mass difference of few tens of eV unknown yet (^{106}Cd, ^{124}Xe, ^{152}Gd, ^{156}Dy, ^{168}Yb, ... [49])
Uncert. in $T_{1/2}^{0\nu}$	Factor ~ 4–9 due to calc. of NME	Many orders in magn. up to measured mass diff. and due to NMEs
Exp. sign.	Peak at end of sum of two el. energy spectra	X rays or Auger el. plus nucl. de-excitation
$T_{1/2}^{0\nu-\exp}$	$> 10^{24}$–10^{25} y	$> 10^{19}$–10^{20} y
Exp. act.	Const. of (0.1–1 ton) exp. with sensitivity to inverted hierarchy of neutrino masses	Small exper. yet
Background	$2\nu\beta\beta$-decay upon resolution of exp.	2νECEC is strongly suppressed

emitted from excited electron shell of the atom. This can be achieved, e.g., by calorimetric measurements. Recently, the most stringent limit on the resonant 0νECEC was established for ^{74}Se [54] and ^{106}Cd [55]. The TGV experiment situated in Modane established limit on the 0νECEC half-life of $1.1 \cdot 10^{20}$ y [55]. Subject of interest was the 0νECEC resonant decay mode of ^{106}Cd (KL-capture) to the excited 2741 keV state of ^{106}Pd. For a long time, the spin value of this final state was unknown and it was assumed to be $J^{\pi} = (1, 2)^{+}$. However, a new value for the spin of the 2741 keV level in ^{106}Pd is $J = 4^{+}$ and this transition is disfavored again due to selection rule.

A comparison of the 0νECEC with the $0\nu\beta\beta$-decay is presented in Table 2. It is maintained that these two lepton number violating processes are quite different and at different levels of both theoretical and experimental investigation. Precise measurements of Q-values between the initial and final atomic states, additional spectroscopic information on the excited nuclear states (energy, spin and parity) and reliable calculation of corresponding NMEs are highly required to improve predictions of half-lives of the resonant 0νECEC. It is expected that the accuracy of 10 eV in the measurement of atomic masses will be achievable in the near future. The electron binding energy depends on the local physical and chemical environment. An interesting question is whether it is possible and, if so, how to manage the atomic structure in such a way as to implement the degeneracy of the atoms and create conditions for the resonant enhancement, as discussed in a recent work [49].

4. SUMMARY

Many new projects for measurements of the $0\nu\beta\beta$-decay have been proposed, which hope to probe effective neutrino mass $m_{\beta\beta}$ down to 10–50 meV. An uncontroversial detection of the $0\nu\beta\beta$-decay will prove the total lepton number to be broken in nature, and neutrinos to be Majorana particles. There is a general consensus that a measurement of the $0\nu\beta\beta$-decay in one isotope does not allow us to determine the underlying physics mechanism. It is very desired that experiments involving as many different targets as possible be pursued. There is also a revived interest in theoretical and experimental study of the resonant 0νECEC, which can probe the Majorana nature of neutrinos and the neutrino mass scale as well. The 0νECEC half-lives might be comparable to the shortest half-lives of the $0\nu\beta\beta$-decays of nuclei provided the resonance condition is matched with an accuracy of tens of electron-volts. There is a lot of theoretical and experiment effort to determine the best 0νECEC candidate.

Nuclear matrix elements of these two lepton number violating processes need to be evaluated with uncertainty of less than 30% to establish the neutrino mass spectrum and CP-violating phases. Recently, there has been significant progress in understanding the source of the spread of calculated NMEs. Nevertheless, there is no consensus among nuclear theorists about their correct values, and corresponding uncertainty. The improvement of the calculation of the nuclear matrix elements is a very important and challenging problem.

Acknowledgements. This work was supported in part by the VEGA Grant agency of the Slovak Republic under contract No. 1/0639/09 and by the Ministry of Education, Youth and Sports of the Czech Republic under contract LM2011027.

REFERENCES

1. *Avignone F. T., Elliott S. R., Engel J.* // Rev. Mod. Phys. 2008. V. 80. P. 481.
2. *Vergados J. D., Ejiri H., Šimkovic F.* arXiv:1205.0649[hep-ph].
3. *Krivoruchenko M. I. et al.* // Nucl. Phys. A. 2011. V. 859. P. 140.
4. *Domin P. et al.* // Phys. Rev. C. 2004. V. 70. P. 065501.
5. *Šimkovic F. et al.* // Phys. Rev. D. 2002. V. 66. P. 033005.
6. *Tretyak V. I., Zdesenko Yu. G.* // At. Data Nucl. Data Tables. 2002. V. 80. P. 83.
7. *Baudis L. et al. (The Heidelberg–Moscow Collab.)* // Phys. Rev. Lett. 1999. V. 83. P. 41.
8. *Tretyak V. I. (The NEMOIII Collab.)* // AIP Conf. Proc. 2011. V. 1417. P. 125.
9. *Arnaboldi C. et al. (The CUORE Collab.)* // Phys. Lett. B. 2004. V. 584. P. 260.
10. *Gando A. et al. (The KamLAND-Zen Collab.).* arXiv:1201.4664[hep-ex].
11. *Auger M. et al. (EXO Collab.)* // Phys. Rev. Lett. 2012. V. 109. P. 032505.
12. *Klapdor-Kleingrothaus H. V., Krivosheina I. V.* // Mod. Phys. Lett. A. 2006. V. 21. P. 1547.
13. *Faessler A. et al.* arXiv:1301.1587[hep-ph].
14. *Pontecorvo B.* // J. Exp. Theor. Phys. 1957. V. 33. P. 549 (Sov. Phys. JETP. 1958. V. 6. P. 429); J. Exp. Theor. Phys. 1958. V. 34. P. 247 (Sov. Phys. JETP. 1958. V. 7. P. 172).
15. *Wendell R. et al. (The Super-Kamiokande Collab.)* // Phys. Rev. D. 2010. V. 81. P. 092004.
16. *Aharmim B. et al. (The SNO Collab.)* // Phys. Rev. C. 2010. V. 81. P. 055504.
17. *Gando A. et al. (The KamLAND Collab.)* // Phys. Rev. D. 2011. V. 83. P. 052002.
18. *Habig A. et al. (The MINOS Collab.)* // Mod. Phys. Lett. A. 2010. V. 25. P. 1219.
19. *Athanassopoulos C. et al.* // Phys. Rev. Lett. 1995. V. 75. P. 2650; 1996. V. 77. P. 3082; 1998. V. 81. P. 1774;
    Auerbach L. B. et al. (LSND Collab.) // Phys. Rev. C. 2001. V. 64. P. 065501.
20. *Aguilar-Arevalo A. A. et al. (MiniBooNE Collab.)* // Phys. Rev. Lett. 2009. V. 102. P. 101802;
    Djurcic Z. (for the MiniBooNE Collab.). arXiv:1201.1519[hep-ex].
21. *Mention G. et al.* // Phys. Rev. D. 2011. V. 83. P. 073006.
22. *Kaether F. et al.* // Phys. Lett. B. 2010. V. 685. P. 47;
    Abdurashitov J. N. et al. // Phys. Rev. C. 2009. V. 80. P. 015807;
    Frekers D. et al. // Phys. Lett. B. 2011. V. 706. P. 134.
23. *Abe Y. et al. (Double Chooz Collab.).* arXiv:1207.6632[hep-ex].
24. *An F. P. et al. (Daya Bay Collab.)* // Phys. Rev. Lett. 2012. V. 108. P. 171803.
25. *Ahn J. K. et al. (RENO Collab.)* // Ibid. P. 191802.
26. *Schwetz T., Tórtola M., Valle J. W. F.* // New J. Phys. 2008. V. 10. P. 113011.
27. *Otten E.W., Weinheimer C.* // Rep. Prog. Phys. 2008. V. 71. P. 086201.
28. *Andreotti E. et al. (MARE Collab.)* // Nucl. Instr. Meth. A. 2007. V. 572. P. 208;
    Nucciotti A. arXiv:1012.2290[hep-ex].
29. *Abazajian K. N. et al.* // Astropart. Phys. 2011. V. 35. P. 177.
30. *Thomas S. A., Abdalla F. B., Lahav O.* // Phys. Rev. Lett. 2010. V. 105. P. 031301.
31. *Maltoni M., Kopp J., Schwetz T.* // Phys. Rev. Lett. 2011. V. 107. P. 091801.
32. *Rodin V. A. et al.* // Phys. Rev. C. 2003. V. 68. P. 044302;
    Rodin V. A. et al. // Nucl. Phys. A. 2006. V. 766. P. 107; 2007. V. 793. P. 213(E).
33. *Šimkovic F. et al.* // Phys. Rev. C. 2008. V. 77. P. 045503.
34. *Menéndez J. et al.* // Nucl. Phys. A. 2009. V. 818. P. 139.

35. *Horoi M., Stoica S.* // Phys. Rev. C. 2010. V. 81. P. 024321.
36. *Fang D. L. et al.* // Ibid. V. 82. P. 051301(R).
37. *Kortelainen M. et al.* // Phys. Lett. B. 2007. V. 647. P. 128;
Kortelainen M., Suhonen J. // Phys. Rev. C. 2007. V. 75. P. 051303; V. 76. P. 024315.
38. *Rath P. K. et al.* // Phys. Rev. C. 2010. V. 82. P. 064310.
39. *Rodriguez T. R., Martinez-Pinedo G.* // Phys. Rev. Lett. 2010. V. 105. P. 252503.
40. *Barea J., Iachello F.* // Phys. Rev. C. 2009. V. 79. P. 044301.
41. *Šimkovic F. et al.* // Phys. Rev. C. 2008. V. 77. P. 045503;
Šimkovic F. et al. // Phys. Rev. C. 2009. V. 79. P. 055501.
42. *Šimkovic F., Faessler A., Vogel P.* // Ibid. V. 77. P. 015502.
43. *Miller G. A., Spencer J. E.* // Ann. Phys. (NY). 1976. V. 100. P. 562.
44. *Winter R.* // Phys. Rev. 1955. V. 100. P. 142.
45. *Vergados J. D.* // Nuc. Phys. B. 1983. V. 218. P. 109.
46. *Bernabeu J., de Rujula A., Jarlskog C.* // Phys. Rev. C. 1983. V. 223. P. 15.
47. *Sujkowski Z., Wycech S.* // Phys. Rev. C. 2004. V. 70. P. 052501.
48. *Douysset G. et al.* // Phys. Rev. Lett. 2001. V. 86. P. 4259;
Blaum K. // Phys. Rep. 2006. V. 425. P. 1;
Blaum K., Novikov Yu. N., Werth G. // Contemp. Phys. 2010. V. 51. P. 149.
49. *Šimkovic F., Krivoruchenko M. I.* // Phys. Part. Nucl. Lett. 2009. V. 6. P. 298;
Krivoruchenko M. I. et al. // Nucl. Phys. A. 2011. V. 859. P. 140.
50. *Eliseev S. et al.* // Phys. Rev. Lett. 2011. V. 106. P. 052504.
51. *Eliseev S. et al.* // Ibid. V. 107. P. 152501.
52. *Šimkovic F., Krivoruchenko M. I., Faessler A.* // Prog. Part. Nucl. Phys. 2011. V. 66. P. 446–451.
53. *Dong-Liang Fang et al.* // Phys. Rev. C. 2012. V. 85. P. 035503.
54. *Frekers D. et al.* // Nucl. Phys. A. 2011. V. 860. P. 1.
55. *Rukhadze N. I. et al.* // Nucl. Phys. A. 2011. V. 852. P. 197.

Received on December 25, 2012.